

Precision Relative Aggregation Number Determinations of SDS Micelles Using a Spin Probe. A Model of Micelle Surface Hydration

Barney L. Bales,* Luis Messina, Arwen Vidal, and Miroslav Peric

Department of Physics and Astronomy and The Center for Cancer and Developmental Biology, California State University at Northridge, Northridge, California 91330-8268

Otaciro Rangel Nascimento

Departamento de Física and Informática, Instituto de Física de São Carlos, Universidade de São Paulo, CEP 13560-970 São Carlos, Brazil

Received: August 13, 1998

A spin-probe method is described that can detect changes in the relative aggregation numbers in SDS micelles with a precision of about one molecule. The method is based on the fact that the ^{14}N hyperfine coupling constant is sensitive to the average fraction of the volume occupied by water in the region of the nitroxide moiety that is located on average near the micelle surface. Defining $A_0(N_A)$ to be the ^{14}N hyperfine coupling constant at an aggregation number N_A , we find $A_0(N_A) = A_0(0) + (\partial A_0/\partial N_A)N_A$, where N_A is controlled by varying either the SDS or the NaCl concentrations. For the spin probe 5-doxylstearic acid ester (5DSE), by combination of the results of experiments in which the SDS and/or the NaCl concentrations were varied, linear least-squares fits gave $A_0(0) = (15.498 \pm 0.009)$ G and $\partial A_0/\partial N_A = -3.99 \pm 0.02$ mG/molecule (constant). $A_0(N_A)$ depends only on the aggregation number despite the fact that a given value of N_A may be prepared by choosing different combinations of NaCl and SDS concentrations. This means that, for a given micelle size, neither interactions between micelles nor the ionic strength of the solution influence the value of A_0 . A geometric model, based on a simple model in which a spherical hydrocarbon core is surrounded by a concentric spherical polar shell, is developed to predict the volume fraction of the polar shell occupied by water as a function of N_A . This water fraction is written in terms of a hydration number per surfactant molecule, $N(\text{H}_2\text{O})$. $A_0(N_A)$ is related to $N(\text{H}_2\text{O})$ by employing the nonempirical polarity index introduced by Mukerjee et al. (Mukerjee, P.; Ramachandran, C.; Pyter, R. A. *J. Phys. Chem.* **1982**, *86*, 3189). The value of $N(\text{H}_2\text{O})$ decreases as the micelle grows because the volume per surfactant molecule in the polar shell decreases. Once $N(\text{H}_2\text{O})$ is specified at a particular value of N_A , no further adjustable parameters enter into the model. The variation with micelle size of the theoretical polarity is in excellent agreement with experiment for values of $N(\text{H}_2\text{O})$ that are comparable to those found from transport properties. The sphere-rod transition is observed as a rather sharp transition in which the detected water volume fraction becomes constant. Detailed future tests of the model are outlined.

Introduction

When prepared from pure surfactants in pure water near the critical micelle concentration (cmc_0) (see Table 1 for nomenclature and abbreviations), most ionic micelles have well-defined aggregation numbers, N_A^0 ; i.e., the size dispersion is small. In the case of SDS, increasing the surfactant concentration^{1–4} or adding salt or a variety of other impurities (see, for example ref 5 and references therein) causes the micelles to grow to larger aggregation numbers, N_A .

For the series of normal sodium alkyl sulfates from octyl to dodecyl, Huisman⁶ found an empirical relationship between N_A and the cmc that was independent of both the alkyl chain length and the concentration of added common counterion. Incorporating results due to Sasaki et al.,⁷ Quina et al.⁸ made the suggestion that this empirical relationship⁶ could be extended to surfactant concentrations above the cmc as follows:

$$N_A = \kappa_2([\text{Na}^+]_{\text{aq}})^\gamma \quad (1)$$

where $[\text{Na}^+]_{\text{aq}}$ is the molar concentration of sodium ion in the aqueous phase whether it is provided by SDS or both SDS and added salt and κ_2 and γ are constants that depend on the alkyl chain length. For SDS, Quina et al.⁸ went on to show that experimental results from a wide variety of techniques fit an equation of the form in eq 1 quite well; however, there was a spread in the values of κ_2 and γ .

The contributions to $[\text{Na}^+]_{\text{aq}}$ from the surfactant and added salt, NaCl in this work, may be found from the conventional pseudophase ion exchange mass balance relationship⁸

$$\begin{aligned} [\text{Na}^+]_{\text{aq}} &= \alpha([\text{SDS}] - [\text{SDS}]_{\text{free}}) + [\text{SDS}]_{\text{free}} + [\text{Na}^+]_{\text{ad}} \\ &= \alpha[\text{SDS}] + \beta[\text{SDS}]_{\text{free}} + [\text{NaCl}] \end{aligned} \quad (2)$$

where the brackets indicate molar concentrations, α is the apparent degree of counterion dissociation, $\beta = 1 - \alpha$, and $[\text{SDS}]_{\text{free}}$ is the concentration of monomeric SDS. The molar

* To whom correspondence should be addressed. E-mail: barney.bales@email.csun.edu.

TABLE 1: Nomenclature and Abbreviations

SDS	sodium dodecyl sulfate
5DSE	nitroxide spin probe 5-doxylstearic acid ester
cmc	critical micelle concentration
cmc ₀	cmc in the absence of added salt or other additives
N_A	number-averaged aggregation number of SDS micelles
N_A^0	number-averaged aggregation number of SDS micelles at the cmc ₀
α	apparent degree of counterion dissociation; $\beta = 1 - \alpha$
$A_0(N_A)$	one-half the difference in the resonance fields of the high- and low-field resonances, neglecting second-order dynamic shifts, equal to the ¹⁴ N hyperfine coupling constant. Also written A_0 .
A_+	difference in the resonance fields of the low- and center-field resonances
A_-	difference in the resonance fields of the high- and center-field resonances
η	second-order shift parameter $\eta = A_- - A_+$
δA_+ , δA_-	second-order dynamic shifts in A_+ and A_- , respectively
τ	rotational correlation time of the nitroxide moiety
$H(25\text{ }^\circ\text{C})$	polarity index ¹⁷ at 25 °C; ratio of the molar concentration of OH dipoles to that in water; for SDS micelles, the number density of water molecules normalized to that in pure water
$[\text{Na}^+]_{\text{aq}}$	molar concentration of sodium ion in the aqueous pseudophase
$[\text{Na}^+]_{\text{ad}}$	molar concentration of added sodium ion; $[\text{Na}^+]_{\text{ad}} = [\text{NaCl}]$ in this paper.
$[\text{SDS}]_{\text{free}}$	molar concentration of monomeric SDS
M_l	projection of the nuclear spin of ¹⁴ N labeling the lines; $M_l = +1, 0,$ and -1 for the low-, center-, and high-field lines, respectively
H_{M_l}	resonance fields of the three lines $M_l = +1, 0,$ and -1
V_{tail}	volume (\AA^3) occupied by one saturated hydrocarbon chain
N_c	number of carbon atoms per chain in the hydrocarbon core
V_p	volume (\AA^3) per surfactant molecule in the polar shell
V_{dry}	volume (\AA^3) per surfactant molecule in the polar shell inaccessible to water
R_c	radius (\AA) of hydrocarbon core
R_m	radius (\AA) of micelle
$N(\text{H}_2\text{O})$	number of water molecules per surfactant molecule in the polar shell; the hydration number
SANS	small-angle neutron scattering
TRFQ	time-resolved fluorescence quenching
X_{MeOH}	weight fraction of methanol in water methanol mixtures
X	molar ratio of 5DSE to SDS
X_m	molar ratio of 5DSE to micellized SDS

concentration of added sodium ion, $[\text{Na}^+]_{\text{ad}}$, is equal to $[\text{NaCl}]$ in this work.

Combining eqs 1 and 2 yields

$$N_A = \kappa_2(\alpha[\text{SDS}] + \beta[\text{SDS}]_{\text{free}} + [\text{NaCl}])^\gamma \quad (3)$$

Defining $N_A^0 = \kappa_2(\text{cmc}_0)^\gamma$, we may rewrite eq 3 as follows:

$$N_A = N_A^0 \left\{ \frac{\alpha[\text{SDS}] + \beta[\text{SDS}]_{\text{free}} + [\text{NaCl}]}{\text{cmc}_0} \right\}^\gamma \quad (4)$$

When $[\text{SDS}] = \text{cmc}_0 = [\text{SDS}]_{\text{free}}$ and $[\text{NaCl}] = 0$, the fraction in the brackets becomes unity and N_A^0 is seen to be the aggregation number at the cmc in the absence of added NaCl.

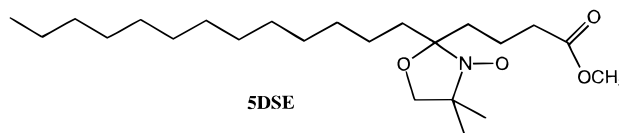
We adopt $\alpha = 0.27$, which is based on reliable activity measurements.⁷ To conform to the values predicted by Quina et al.,⁸ we also adopt the values $\kappa_2 = 164$ and $\gamma = 1/4$ as derived from Huisman's empirical equation.⁶ Using $\text{cmc}_0 = 0.0083$ M results in $N_A^0 = 49.5$. Thus, eq 4 becomes

$$N_A = 49.5 \left\{ \frac{0.27[\text{SDS}] + 0.73[\text{SDS}]_{\text{free}} + [\text{NaCl}]}{0.0083} \right\}^{0.25} \quad (5)$$

In writing eq 5, we have tacitly assumed that β is constant, which has only been demonstrated up to values of $[\text{SDS}] = 80$ mM. Small variations in β would not be easy to detect in direct measurements of N_A given the uncertainties in the various methods, especially at large SDS concentrations. We employ eq 5 as a convenient method to present the results and show below that the conclusions of this work are the same whether we use eq 5 or directly measured values of N_A . Values of $[\text{SDS}]_{\text{free}}$ are calculated iteratively from eq 5 of ref 8.

The motivation for the present work arose from observations^{9,10} that the isotropic hyperfine coupling constant, A_0 , of

the nitroxide spin probe 5-doxylstearic acid ester (5DSE) varied



linearly with $[\text{SDS}]^{1/4}$. Bezzobotnov et al.,² on the basis of small-angle neutron scattering (SANS) experiments, had suggested that N_A varied linearly with $[\text{SDS}]^{1/4}$, leading us to speculate⁹ that measurements of A_0 might lead to an easy, precise method to investigate N_A . Note that the proposed² $[\text{SDS}]^{1/4}$ dependence of N_A in the absence of NaCl is identical to eq 4 with $\gamma = 1/4$ but excluding the term involving $[\text{SDS}]_{\text{free}}$. The difference in the dependence of N_A vs $[\text{SDS}]$ including or excluding $[\text{SDS}]_{\text{free}}$ only becomes apparent at surfactant concentrations approaching cmc_0 . The derivation of eq 3 as presented in ref 8, experimental data,⁸ and the results given in this work all favor the inclusion of $[\text{SDS}]_{\text{free}}$.

It is well-known that A_0 for a nitroxide spin probe such as 5DSE varies systematically with the solvent polarity,¹¹⁻¹³ so the previous work^{9,10} showed that as the micelle grew because of increasing $[\text{SDS}]$, the polarity sensed by 5DSE decreased.

The first purpose of the present work is to show that this behavior is true whether the size is varied by changing the surfactant or the salt concentrations; i.e., A_0 is the same for a given value of N_A even if this aggregation number is attained using different combinations of $[\text{SDS}]$ and $[\text{NaCl}]$. This purpose seems worth pursuing for two reasons. (1) A_0 is a simple quantity to measure with high precision. With modern magnet power supplies and controllers providing reproducible, linear magnetic field sweeps and with spectral fitting techniques,^{14,15} A_0 may be measured with a relative precision of at least 2 orders-of-

magnitude better than measurements of N_A itself. Thus, it potentially offers a simple method to detect small changes in N_A . (2) The theoretical basis for variations in A_0 is well understood;^{13,16–23} therefore, the method could lead to a model that provides better insight into the local structure of the solubilization site of the spin probe.

The second purpose of the work is to propose such a model for the surface hydration of the SDS micelle. The suitability of the use of the solvatochromic properties of nitroxide free radicals for studying lipid assemblies such as micelles has been critically discussed by Mukerjee and co-workers.^{16–18} See refs 13, 16–21, 23, and 24 and references therein for thorough discussions of the mechanisms leading to the solvatochromic properties. Mukerjee et al.¹⁷ introduced a nonempirical polarity scale that showed excellent linear correlation with values of A_0 for two nitroxide spin probes. The scale, referred to as a polarity index and denoted by $H(25\text{ }^\circ\text{C})$ by those authors,¹⁷ is defined to be the ratio of the molar concentration of OH dipoles in a solvent or solvent mixture to that in water. $H(25\text{ }^\circ\text{C})$ shows good linear correlation with other measures of polarity,¹⁷ such as the dielectric constant, with the obvious advantage that it is a straightforward matter to calculate the index from molecular structures and densities. Provided that the solvent mixture of interest is water and molecules possessing no OH bonds, $H(25\text{ }^\circ\text{C})$ is simply the volume fraction occupied by water.

The growth of the SDS micelles is accompanied by an increase in their size dispersion,²⁵ which, in principle, requires a distinction between number- or mass-averaged aggregation numbers. The two averages are related as follows: $N_m = N_n + \sigma_n^2/N_n$, where the subscripts m and n denote mass-averaged and number-averaged aggregation numbers, respectively, and σ_n is the dispersion in the number. In practice, this dispersion reaches about 22 molecules for $[\text{SDS}] = 70\text{ mM}$ and $[\text{NaCl}] = 400\text{ mM}$, leading to a maximum difference in the two averages of less than four molecules.²⁵ All of our measurements from which we derived quantitative results lie within this range. Since the uncertainties in N_A are on the order of five molecules (see below), we ignore the difference in the two averages. The aggregation numbers of SDS micelles are also temperature-dependent.^{1,2,26} Combining results from TRFQ^{1,26} and SANS,² $\partial N_A/\partial T = -0.50 \pm 0.31$ molecules/ $^\circ\text{C}$. Therefore, correction to $25\text{ }^\circ\text{C}$ for aggregation numbers measured at 20 and $21\text{ }^\circ\text{C}$ would involve corrections of only two to three molecules that are ignored. Thus, all aggregation numbers quoted from the literature are the original uncorrected values.

Methods and Materials

Sigma molecular biology reagent SDS, 99% (lot no. 46F-0543), was used as received. The surface tension, derived from the drop-volume method, vs concentration plot of this reagent, given in Figure 1 of ref 3, showed no minimum near the cmc. Distilled water was purchased from Arrowhead. Sodium chloride 99+% A.C.S. reagent was purchased from Aldrich and used as received. A solution of 5DSE (Sigma, as received) in methanol (Spectrum, reagent, A.C.S., as received) was distributed to vials by weight, dried with a stream of nitrogen gas, capped, and stored in the freezer until needed.

After a vial was warmed to room temperature, SDS and water were added to prepare a mother solution of the desired concentrations of SDS and 5DSE. This sample was gently stirred for several hours before adding further distilled water and/or adding salt to the mother solution to produce a series of samples in which $[\text{SDS}]$ or $[\text{NaCl}]$ was varied, respectively. This method of sample preparation ensures a constant spin-

probe/surfactant molar ratio whether $[\text{SDS}]$ or $[\text{NaCl}]$ is varied, thus minimizing the effect of variations of spin exchange interactions (see Appendix). After being gently stirred for a few more minutes, the samples, not degassed, were drawn into glass capillaries and sealed with a gas torch. The sample capillary was then placed within a quartz tube, which was placed in the Dewar within the cavity. The temperature was controlled with a Bruker nitrogen flow unit to $\pm 0.1\text{ }^\circ\text{C}$ and measured with a thermocouple placed just above the cavity in position C of Figure 1 of ref 27.

The rationale for using the spin probe 5DSE has been discussed in previous work.^{9,10} Details of the effect of varying the spin-probe concentration are given in the Appendix.

EPR spectra were mostly taken at X-band using a Bruker 300ESP spectrometer. A large modulation amplitude of 1 G was employed, taking advantage of the fact²⁸ that only the inhomogeneous (Gaussian) component is broadened. At low modulation amplitudes, 5DSE has a Gaussian line width in SDS micelles of $0.80 \pm 0.02\text{ G}$, independent of the aggregation number. The Gaussian line width averaged over the central lines of all the spectra in this study was found to be $\Delta H_{\text{pp}}^{\text{G}} = 0.94 \pm 0.02$; thus, the modulation broadened the Gaussian component by $0.49 \pm 0.03\text{ G}$, in excellent agreement with a recent study²⁹ showing that the Gaussian component is broadened (in quadrature) by $H_m/2$ where H_m is the peak-to-peak value of the modulation amplitude. A few spectra were taken at L-band (1.28 GHz) using a home-built bridge, a loop-gap resonator,³⁰ and a Varian magnet. The field sweep of the magnet, described previously,³⁰ was calibrated with a 0.1 mM solution of Fremy's salt in 50 mM potassium carbonate using the recently redetermined²⁷ hyperfine coupling constant of 13.056 G at $25\text{ }^\circ\text{C}$.

Results

Figure 1 shows EPR spectra of 5DSE in 500 mM SDS at $25\text{ }^\circ\text{C}$ measured at X-band (9.42 GHz, Figure 1a) and L-band (1.28 GHz, Figure 1b). The resonance fields of the lines were established by fitting the spectra to a Gaussian–Lorentzian sum function as described previously.¹⁴ We showed previously²⁷ that, for low-noise spectra, this procedure reproduces the positions at which the first derivative lines crossed the baseline to better than 1 mG, provided linear interpolation between data points is used. A Bruker NMR Gaussmeter was used in the 1 mG resolution range to measure the sweep width of each spectrum. In an experiment spanning an hour or two, the 50 G sweep width was reproduced to about 3–4 mG. A mean value of the sweep width in any one run was used to compute A_0 , which is taken to be one-half the difference in the resonance fields of the high- and low-field lines, in gauss. Note that values of A_0 are reproduced to within about 1–2 mG despite the fact that the interval between consecutive points is on the order of 12 mG.

For the spectrum in Figure 1a, at X-band, $A_0 = 15.100 \pm 0.002\text{ G}$, and in Figure 1b, at L-band, $A_0 = 15.099 \pm 0.008\text{ G}$, where the error at X-band represents standard deviations from five spectra using the same sample. The uncertainty at L-band is dominated by corrections for magnetic field-sweep nonlinearities.²⁷ We define the spacings between hyperfine lines as $A_+ = H_0 - H_{+1}$ and $A_- = H_{-1} - H_0$, where H_{M_1} denotes the resonance fields of the three lines: $M_1 = +1, 0,$ and -1 corresponding to the low-, center-, and high-field lines, respectively (see Figure 1). Measurements of the second-order shift parameter yield $\eta = A_- - A_+ = -0.035 \pm 0.001\text{ G}$ for the spectrum in Figure 1a, which is to be compared with the static

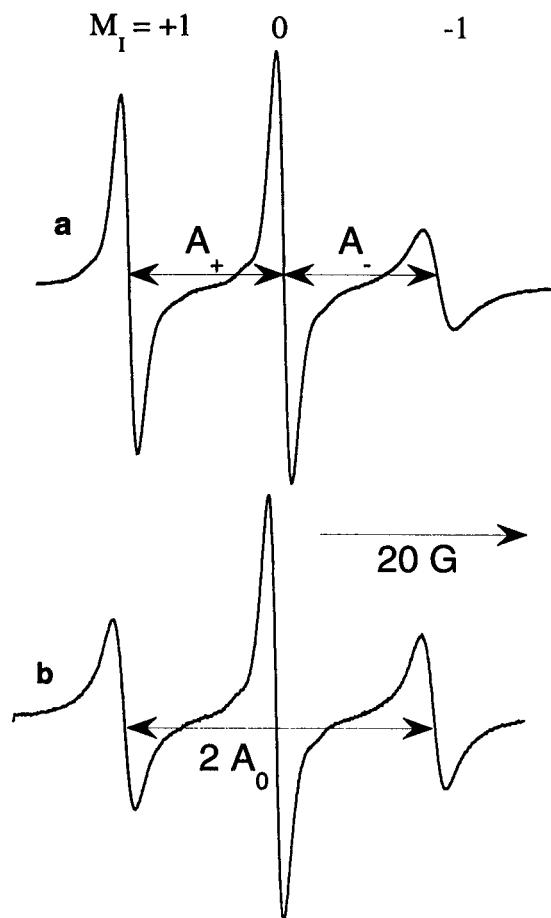


Figure 1. EPR spectra of 5DSE in 500 mM SDS micelles without added salt at (a) X-band and (b) L-band. The definitions of the hyperfine spacings A_0 , A_+ , and A_- are shown. The values of A_0 at X- and L-band are the same within experimental error.

shift of $A_0^2/H_0 = 0.068$ G; thus, a departure from the static shift is observed. This type of asymmetry is commonly observed in nitroxide spectra^{31–33} as the rotational mobility slows. This asymmetry is dominated by a shift of the high-field line ($M_1 = -1$) toward the center as the rotational correlation time increases in response to decreasing temperature.^{31–33} Denote the shift in A_+ and A_- with rotational correlation time by δA_+ and δA_- respectively. In an 85% glycerol/D₂O solution³² experimental values of $\delta A_+ = -0.01$ G and $\delta A_- = -0.41$ G were found as the temperature was decreased from 26.1 to 11.2 °C over which range τ_R increased from 0.32 to 1.1 ns. Theoretical calculations ranged from $\delta A_+ = 0$ to -0.007 and $\delta A_- = -0.22$ to -0.46 G over this same temperature range depending upon model employed.^{31,32} Thus, experimentally and theoretically, δA_+ is small, about an order of magnitude smaller than δA_- , and on the order of the experimental uncertainties. We therefore neglect the shift δA_+ . To estimate the uncertainty in neglecting δA_+ , we note that the rotational correlation time reaches a maximum of $\tau = 0.84$ ns when SDS is varied over the range $[\text{SDS}] = 25\text{--}200$ mM.¹⁰ Using appendix C of ref 32 for $\tau = 0.84$ ns, we calculate $\delta A_+ = -4$ mG. This uncertainty would introduce a relative uncertainty in the value of $H(25^\circ)$ calculated from eq 8 below of less than 0.003, negligible compared with other sources of uncertainty.

Our experiments are at constant temperature; however, as the micelle grows, the rotational correlation time increases;¹⁰ thus, the magnitude of δA_- increases, which means that the operational definition of A_0 decreases faster than the true hyperfine

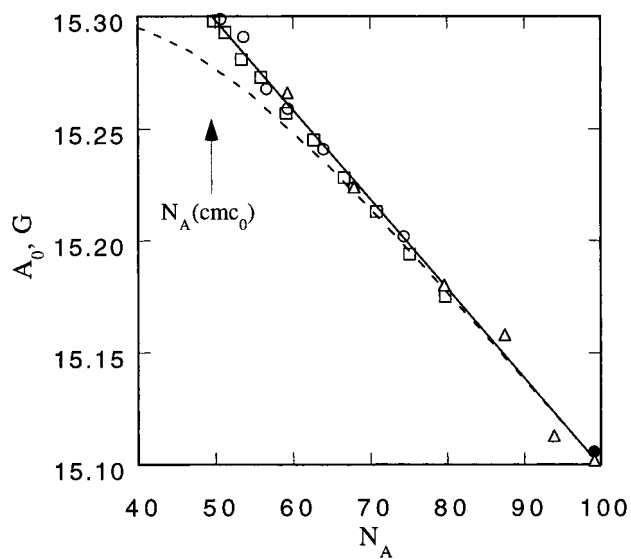


Figure 2. A_0 as a function of aggregation number by varying the SDS concentration for three typical runs at X-band (open symbols) and the measurement derived from Figure 1b at L-band (filled circle). These data cover a very wide range of SDS concentrations from just above the $\text{cmc}_0 = 8.3$ to 500 mM. The reproducibility is generally less than the size of the symbols; however, the correction for spin-probe concentration (Appendix) is about twice the size of the symbols near the cmc_0 . The straight line is the average of linear least-squares fits to all experiments, i.e., by varying either the SDS or the NaCl concentrations. The dashed line is the same linear fit, however, plotted against the aggregation number calculated from eq 5 by neglecting the term $[\text{SDS}]_{\text{free}}$, showing a severe departure from linearity at low aggregation numbers. The aggregation at the cmc_0 , $N_A^0 = 49.5$, is indicated.

coupling constant. Therefore, part of the decrease in A_0 is due to decreased polarity and part due to the dynamic shift δA_- .

We have two related but different objectives in this work. The first is to provide a rapid, precise method of determining the relative aggregation numbers of SDS micelles. The second is to demonstrate that a simple model gives a satisfactory account of the observations. To achieve the first, we have chosen to report the variation of A_0 with N_A because A_0 is the quantity most familiar to experimentalists and A_0 varies linearly with N_A . The same conclusions would be reached were we to report A_+ vs N_A ; however, A_+ does not vary linearly with N_A , making the calculations more complicated. To achieve the second objective, we capitalize on the fact that δA_+ is small and use A_+ to compare the experimental polarity with a model.

Second-order dynamic shifts for nitroxides are predicted³⁴ to be weakly dependent upon microwave frequency in the range of rotational correlation times pertinent to 5DSE in SDS. This seems to be the case, since the measurements in Figure 1, taken at 9.42 and 1.28 GHz, yield a negligible discrepancy in A_0 .

The EPR spectrum of 5DSE in SDS micelles is an excellent Voigt shape with inhomogeneous broadening (Gaussian line width) equal to that in homogeneous solvents.³⁵ This means that the environment reported by this spin probe is an effective environment averaged by the rapid, almost isotropic motion of the NO moiety.¹⁰ A static distribution of the spin probe in different regions of the micelle would lead to further inhomogeneous broadening, which would be easily detected and is not observed.

Dependence of A_0 upon N_A . Figure 2 shows the results of three typical experiments at X-band in which the concentration of SDS was varied from just above the $\text{cmc}_0 = 8.3$ mM to near 500 mM in the absence of added NaCl. Also included in Figure 2 is the datum (filled circle) from the spectrum in Figure

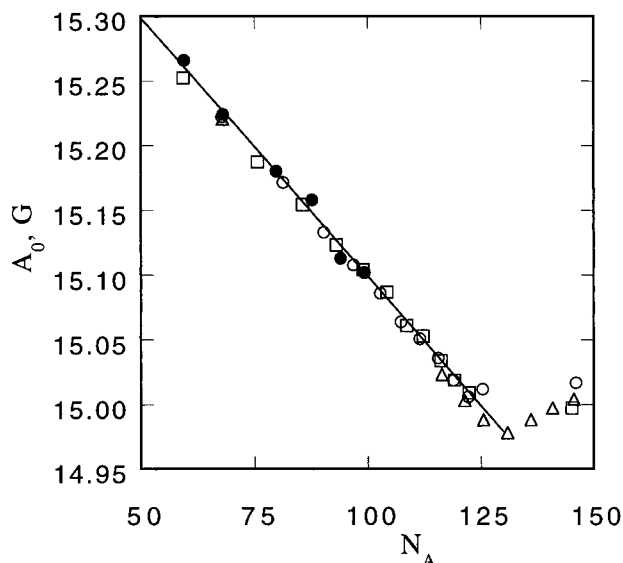


Figure 3. A_0 as a function of aggregation number by varying the NaCl concentration for 50 mM SDS (\square and \triangle) and 100 mM SDS (\circ). For comparison, one run varying the SDS concentration is included (\bullet). The straight line is the average of linear least-squares fits to all experiments, i.e., by varying either the SDS or the NaCl concentrations. The rather abrupt departure from linearity at about $N_A = 130$ is attributed to the sphere-rod transition.

TABLE 2: Summary of Experiments and Linear Least-Squares Fits to Eq 6^a for the Spin Probe 5DSE in SDS with N_A Computed from Eq 5 ($T = 25.0$ °C)

[SDS] mM	[NaCl] mM	$A_0(0)$ G	$\partial A_0/\partial N_A$ mG/molecule	r^b
25–200 ^c	0		-3.96 ± 0.12	0.999(4)
50–495	0	15.508 ± 0.005^d	-4.11 ± 0.20	0.995(6)
50–200	0	15.491 ± 0.005^e	-4.03 ± 0.05	0.999(3)
9.4–200	0		-4.08 ± 0.04	0.999(10)
12.5–200	0		-4.16 ± 0.20	0.994(7)
100	0–317	15.495 ± 0.003^d	-4.04 ± 0.03	0.999(4)
100	0–249		-3.92 ± 0.03	0.999(9)
50	0–265		-3.81 ± 0.06	0.999(10)

^a Errors calculated from the least-squares fit to eq 5. ^b Coefficient of correlation using the number of experimental points indicated in the parentheses. ^c Data from ref 9. ^d Field sweep calibrated with NMR gauss meter. ^e Fremy's salt.²⁷

1b measured at L-band. In Figure 2, A_0 is plotted vs N_A as calculated from eq 5. The reproducibility is generally less than the size of the symbols; however, the correction for spin-probe concentration (see Appendix) is about twice the size of the symbols near the cmc₀. The straight line is the average of linear least-squares fits to *all* experiments, i.e., those in Figure 2 in which [SDS] is varied and those in Figure 3 and others in Table 2 in which [NaCl] is varied. The dashed line is the same linear fit, however, plotted against the aggregation number calculated from eq 5 by neglecting the term $[\text{SDS}]_{\text{free}}$, showing a severe departure from linearity at low aggregation numbers. The aggregation number at the cmc₀, $N_A^0 = 49.5$, is indicated in Figure 2. Figure 2 shows that A_0 vs N_A continues to be linear with the same slope to very high detergent concentrations. Table 2 details the eight experiments carried out in this work.

Figure 3 shows the results of three experiments in which the salt concentration was varied with [SDS] fixed and, for comparison, one in which the detergent concentration was varied. Clearly, the variation of A_0 with N_A is the same whether salt is added or detergent increased. For example, the datum indicated by the filled circle near $N_A = 99$ is derived from [SDS] = 500 mM [NaCl] = 0 while the open square that is almost

TABLE 3: Fits of A_0 to Eq 6 for the Spin Probe 5DSE in SDS Micelles Using Experimental Values of N_A Taken from the Literature

technique	$A_0(0)$ G	$\partial A_0/\partial N_A$ mG/molecule	r^b	ref
light scattering ^c	15.539	-4.33	0.996(5)	6
ultracentrifugation ^d	15.516	-4.26	0.991(3)	36
SANS ^e	15.431	-3.96	0.949(7)	37
TRFQ ^{f,g}	15.470	-3.79	0.993(5)	38
TRFQ ^{f,h}	15.483	-3.45	0.976(4)	4
mean	15.488 ± 0.042	-3.96 ± 0.35		

^a A_0 measured at 25.0 °C. ^b Coefficient of correlation with the number of points in the parentheses. ^c At 21 °C. ^d Corrected by isopiestic distillation, 25 °C. ^e Small-angle neutron scattering, 25 °C. ^f Time-resolved fluorescence quenching. ^g Pyrene excimer quenching, 25 °C. ^h Pyrene quenched by methyl viologen, 20 °C, with values of N_A recalculated using $[\text{SDS}]_{\text{free}}$ rather than cmc₀.

coincident with the filled circle is derived from [SDS] = 50 mM and [NaCl] = 118 mM.

The linear portions of the curves were fit to straight lines as follows:

$$A_0(N_A) = A_0(0) + \frac{\partial A_0}{\partial N_A} N_A \quad (6)$$

The results are tabulated in Table 2. Within the experimental uncertainties, the slopes of the linear curves are not affected by the correction for spin-probe concentration detailed in the Appendix. The values of $A_0(0)$ were corrected using eq 17 of the Appendix; however, only those requiring less than 6 mG correction are included in Table 2. The mean values computed from the results in Table 2 inversely weighted by their own variance are $A_0(0) = 15.498 \pm 0.009$ G and $\partial A_0/\partial N_A = -3.99 \pm 0.02$ mG/molecule. The straight lines in Figures 2 and 3 are plots of eq 6 with these values.

The numerical values of $A_0(0)$ and $\partial A_0/\partial N_A$ in eq 6 depend on the values of N_A , which have, thus far, been calculated using eq 5 employing a constant value of β . The following question arises. To what extent does using the empirical form of eq 4, and specifically using the particular parameters in eq 5, affect the results? To explore this question, we turn to some literature^{4,6,36–38} values of N_A measured by a variety of techniques over a wide range of values of $[\text{Na}^+]_{\text{aq}}$. We proceed by fitting our results to an empirical function of $[\text{Na}^+]_{\text{aq}}$, yielding the following:

$$A_0 = 15.498 - 0.654\{[\text{Na}^+]_{\text{aq}}\}^{0.25} \quad (7)$$

Plots of our results as a function of $\{[\text{Na}^+]_{\text{aq}}\}^{0.25}$ are identical in form to Figures 2 and 3; however, now no reference is made to an assumed value of N_A . Equation 7 allows us to interpolate values of A_0 that would be measured under the conditions of the experiments taken from the literature. Five sets of values of N_A were taken from the literature.^{4,6,36–38} For each value of N_A , eq 7 was used to calculate the value of A_0 from the corresponding value of $[\text{Na}^+]_{\text{aq}}$. These literature values of N_A were then fit to a linear equation of the form of eq 6. The results of these fits are presented in Table 3. The coefficients of correlation show that A_0 is a good linear function of directly measured values of N_A . The unweighted means from the five experiments yield $A_0(0) = 15.488 \pm 0.042$ G and $\partial A_0/\partial N_A = -3.96 \pm 0.35$ mG/molecule, where the uncertainties are the standard deviations. Thus, both $A_0(0)$ and $\partial A_0/\partial N_A$ are found to be the same within experimental error whether derived

TABLE 4: Fits to Eq 4 of Experimental Values of N_A Taken from the Literature ($\alpha = 0.27^a$)

technique	N_A^0	γ	cmc ₀ M	r^a	ref
eq 5 ^b	49.5	0.25	0.0083		8
light Scattering ^c	51.9	0.212	0.00814	0.995(5)	6
ultracentrifugation ^d	50.1	0.236	0.0082	0.996(3)	36
SANS ^e	44.8	0.214	0.0083	0.987(7)	37
TRFQ ^{f,g}	47.3	0.259	0.0083	0.995(5)	38
TRFQ ^{f,h}	54.2	0.247	0.0083	0.978(4)	4

^a Coefficient of correlation with the number of points in the parentheses. ^b Best fit to sodium octyl, nonyl, decyl, undecyl, and dodecyl sulfate at $T = 21$ °C. ^c At 21 °C. ^d Corrected by isopiestic distillation, 25 °C. ^e Small-angle neutron scattering, 25 °C. ^f Time-resolved fluorescence quenching. ^g Pyrene excimer quenching, 25 °C. ^h Pyrene quenched by methyl viologen, 20 °C, with values of N_A recalculated using $[\text{SDS}]_{\text{free}}$ rather than cmc_0 .

directly from measured values of N_A or from eq 5. The conclusion is that eq 6 gives the correct dependence of A_0 on N_A with an uncertainty dominated by the known values of N_A .

In Table 4, we present the fits of some literature values of N_A to eq 4 holding β constant. The fits to eq 4 are rather good, which shows that eq 4 is a good empirical description of the aggregation numbers of SDS even at surfactant concentrations above the cmc; however, there is a scatter in the absolute value of the aggregation number. For example, the unweighted mean value and the standard deviation of the results in Table 2 at the cmc_0 are $N_A^0 = 50 \pm 4$. Equation 4 is also a good empirical description of the results of other experiments.⁸ Note that the precision of the experiments to date is not sufficient to decide whether β is constant or not; therefore, allowing β to vary as an adjustable parameter is not yet justified.

In Figure 3, at higher values of $[\text{Na}^+]_{\text{aq}}$, one observes a rather sharp departure from linearity at about $N_A = 130$ ($[\text{Na}^+]_{\text{aq}} \approx 400$ mM), indicating that the polarity sensed by 5DSE no longer decreases with added salt or surfactant. Many authors^{37–40} have observed a sudden increase of micelle size at $[\text{NaCl}] = 400–450$ mM ($N_A = 130–134$, eq 5) attributed to a sphere–rod transition.^{39,40} Thus, we attribute the transition in Figure 3 to the sudden increase in growth of the micelles and refer to this as the sphere–rod transition. Note that eq 5 no longer holds above the sphere–rod transition point, so the values of N_A that are plotted near 140–150 are in reality micelles with much larger aggregation numbers,^{37,40} thus, the transition is even sharper than it appears in Figure 3.

We did not study any possible aging effects over short time spans. Typically, a sample was measured the day after it was first prepared. Comparing the results from a sample with $[\text{SDS}] = 200$ mM and $[\text{NaCl}] = 0$ after 1 day and 2 months showed identical values of A_0 .

In the case of 5DSE, by use of the operational definition of A_0 , the variation of A_0 with N_A is linear, so $\partial A_0 / \partial N_A$ is a constant. Preliminary work using other spin probes and measurement of 5DSE at L-band reveal slight curvatures in the variations of A_0 with N_A .

Dependence of A_+ on the Polarity Index H

The value of A_+ (rather than A_0 to minimized the effects of the second-order dynamics shifts) was measured as a function of polarity. Solutions of 5DSE (0.05 mM) were prepared in a series of mixtures of methanol and water.¹⁷ For each mixture, the value of the polarity index $H(25$ °C) was calculated from a linear least-squares fit of the data given in Table 1 of Mukerjee et al.¹⁷ for water/methanol mixtures at 25 °C as follows:

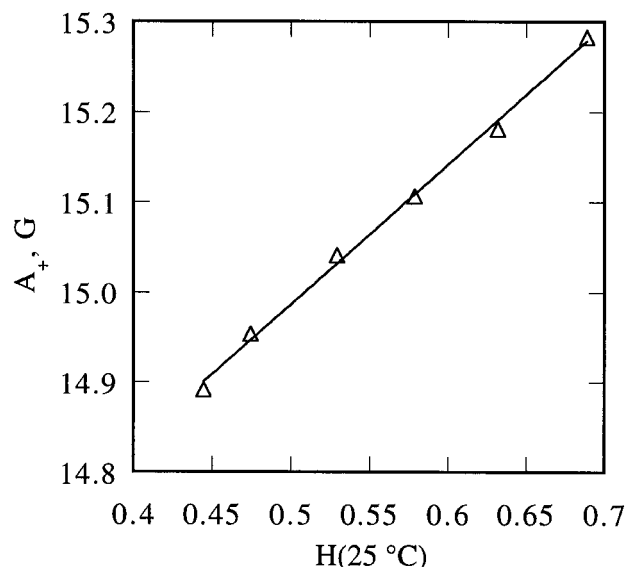


Figure 4. A_+ as a function of the polarity index $H(25$ °C) in a series of methanol water mixtures. The straight line is a linear least-squares fit to the data.

$H(25$ °C) = $0.987 - 0.542X_{\text{MeOH}}$, where X_{MeOH} is the weight fraction of methanol. This linear fit deviates by a maximum of 0.4% from the correct values over the range $H(25$ °C) = 0.446–0.828, which corresponds to $X_{\text{MeOH}} = 1.0–0.3$.

The mean values of five measurements of A_+ in each mixture are shown in Figure 4 versus $H(25$ °C). The standard deviations are smaller than the symbols. Fitting the data to

$$A_+(H) = A_+(0) + \frac{\partial A_+}{\partial H} H(25$$
 °C) (8)

yields $A_+(0) = 14.210 \pm 0.025$ G and $F(\partial A_+ / \partial H) = 1.552 \pm 0.044$ G with coefficient of correlation $r = 0.998$ over the range $H(25$ °C) = 0.44–0.69. Most of the measurements leading to eq 8 were made at room-temperature $T = 26.7 \pm 0.3$ °C. Previously, we found²⁷ that A_0 only varies by about 0.2 mG/°C, so corrections to 25 °C are negligible, and a few measurements at 25.0 °C confirmed this fact.

Dependence of the Polarity Index $H(25$ °C) on the Aggregation Number N_A

Figure 5 shows the results of computing values of the polarity index $H(25$ °C) in SDS micelles from measured values of A_+ for two of the experiments. The results of all of the experiments fall very near those in Figure 5 with scatter similar to that in Figures 2 and 3.

It is important to note that electric fields near the surface of the micelle are not expected to influence the value of A_+ , since rapid rotation of the nitroxide moiety averages the effects of these fields.¹⁹

Hydration Model

We construct a simple model based on a classical picture of the micelle as having a hydrocarbon core with very little water penetration.⁴¹ Drawing upon the work of Mukerjee and co-workers,¹⁸ we suppose that the spin probe is adsorbed onto the micelle surface. The spin probe 5DSE is known to execute rapid, almost isotropic motion in an SDS micelle;⁴² thus, we suppose that the nitroxide moiety randomly and rapidly samples all portions of the polar layer surrounding the hydrocarbon core.

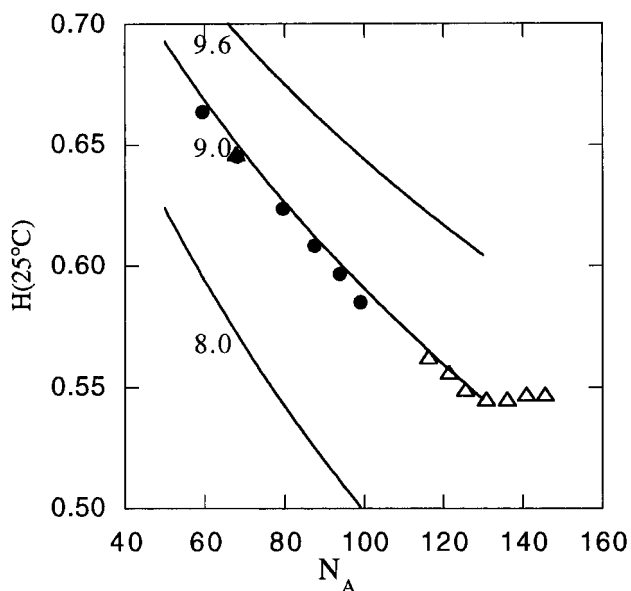


Figure 5. Experiment values of the polarity index $H(25^\circ\text{C})$ of the SDS micelle surface as measured by the spin-probe 5DSE versus the aggregation number. Only two of the experiments are shown for clarity; the others overlay these data with scatter similar to that in Figures 2 and 3. The solid lines are calculated from the geometrical hydration model described in the text. The numbers next to the solid lines indicate the number of water molecules per surfactant molecule at the reference size of $N_A = 63$.

We propose that the physical basis for the decrease in A_0 (and A_+) with micelle size is due to a dehydration (per surfactant molecule) of the micelle surface as the micelle grows. This is a simple geometric effect: as the micelle grows, the area per headgroup decreases, leaving less room for water molecules. Decreasing water content would lead to a decreasing polarity that would decrease A_0 . For a discussion of micelle hydration, see ref 41 and references therein. We note that essentially this mechanism was advanced many years ago by Lianos and Zana³⁸ to account for the systematic increase in the relative intensities of the third to first vibronic bands in the fluorescence emission spectrum of pyrene.

We assume (1) that a simple two-shell spherical model,⁴³ with a hydrocarbon core and a polar shell, is adequate to describe the hydration of the polar shell. Additionally, we assume (2) the nitroxide moiety of 5DSE resides in the polar layer, undergoing rapid rotational motion that allows the nitroxide to sample all regions of the layer and report the average polarity. Finally, we assume (3) that the thickness of the polar shell is approximately constant as the micelle grows. This assumption has been previously employed in the interpretation of SANS experiments³⁷ and seems to be reasonable, since the thickness of the polar shell ($\sim 5 \text{ \AA}$)⁴³ is approximately equal to the diameter of the SO_4Na headgroup.⁴⁴

In this model, the micelle is composed of an inner spherical hydrocarbon core of radius R_c and an outer concentric polar shell of thickness $R_m - R_c$ where R_m is the radius of the micelle. The core contains the hydrocarbon tails of the surfactant molecules, except perhaps for the first methylene group, and the polar shell contains the headgroups (OSO_3^-), a fraction β of the counterions (Na^+), and water. An ellipsoid of revolution is often employed,^{45–47} a sphere being a special case.⁴³ Thus, the geometry of the micelle is characterized by the radius of the hydrocarbon core, R_c , and the radius of the micelle, R_m . The volume of the core is taken to be $N_A V_{\text{tail}}$, where V_{tail} is the volume occupied by the saturated hydrocarbon chain, calculated according to Tanford (p 52 of ref 48) as

$$V_{\text{tail}} = 27.4 + 26.9N_c \quad (9)$$

where V_{tail} is in units of \AA^3 and N_c is the number of carbon atoms per chain that are embedded in the micelle core. Thus, the core radius is found from

$$N_A V_{\text{tail}} = \frac{4\pi}{3} R_c^3 \quad (10)$$

The volume per surfactant molecule in the polar shell, V_p , is given by

$$V_p = \frac{4\pi}{3N_A} (R_m^3 - R_c^3) \quad (11)$$

There is disagreement in the literature about how many methylene groups are “wet”, i.e., what the value of N_c ought to be. We take $N_c = 12$, in keeping with adopting the simplest approach, yielding $V_{\text{tail}} = 350 \text{ \AA}^3$, which compares well with Cabane’s estimate of 346 \AA^3 .⁴⁴ The SANS results of Cabane⁴³ showed that the thickness of the polar shell is $R_m - R_c \approx 5 \text{ \AA}$.

We denote the average number of water molecules residing in V_p by $N(\text{H}_2\text{O})$, which we refer to as the hydration number per surfactant molecule. Taking the volume per water molecule to be 30 \AA^3 ,⁴⁴ the volume fraction of V_p occupied by water is given by

$$H = 30N(\text{H}_2\text{O})/V_p \quad (12)$$

where V_p is in units of \AA^3 .

There have been a number of investigations^{41,49–52} of the hydration of SDS micelles, so ideally, we would fix the value of $N(\text{H}_2\text{O})$ from other measurements and proceed with no adjustable parameters. Unfortunately, the estimates of $N(\text{H}_2\text{O})$ vary between 8 and 12 when derived from hydrodynamic measurements⁴¹ and much larger values have been suggested.⁵² The previous models do not take into account the fact that $N(\text{H}_2\text{O})$ could vary as the micelles grow, so an average value of $N(\text{H}_2\text{O})$ would emerge. Our model predicts a decrease in the value of $N(\text{H}_2\text{O})$ as the micelle grows, so one needs to specify $N(\text{H}_2\text{O})$ at a particular value of N_A and then compute $N(\text{H}_2\text{O})$ as a function of N_A .

Let us illustrate by using as a reference the 69 mM SDS system employed by Cabane,⁴³ who suggested $N(\text{H}_2\text{O}) = 8$. According to eq 5, $N_A = 63$, and evaluating eqs 10 and 11 gives $V_p = 397 \text{ \AA}^3$. If we divide V_p into the volume occupied by water and a volume inaccessible to water, V_{dry} , then

$$N(\text{H}_2\text{O}) = (V_p - V_{\text{dry}})/30 \quad (13)$$

Inserting $V_p = 397 \text{ \AA}^3$ yields $V_{\text{dry}} = 157 \text{ \AA}^3$.

The same calculations for $N(\text{H}_2\text{O}) = 9$ at $N_A = 63$ gives $V_{\text{dry}} = 127 \text{ \AA}^3$, and for $N(\text{H}_2\text{O}) = 9.6$, they lead to $V_{\text{dry}} = 109 \text{ \AA}^3$. For comparison, the volume occupied by the sodium sulfate headgroup is about 66.4 \AA^3 ,⁴⁴ somewhat smaller than V_{dry} from these estimates of $N(\text{H}_2\text{O})$. Insisting on a value of $V_{\text{dry}} = 66.4 \text{ \AA}^3$ leads to $N(\text{H}_2\text{O}) = 11.0$ at $N_A = 63$. It is important to note that one may specify either V_{dry} or the value of $N(\text{H}_2\text{O})$ for a given value of N_A to fix the model.

The value of the polarity parameter, combining eqs 12 and 13, is given by

$$H = (V_p - V_{\text{dry}})/V_p \quad (14)$$

To avoid an adjustable parameter, we make the reasonable assumption that as the micelle grows, the inaccessible volume

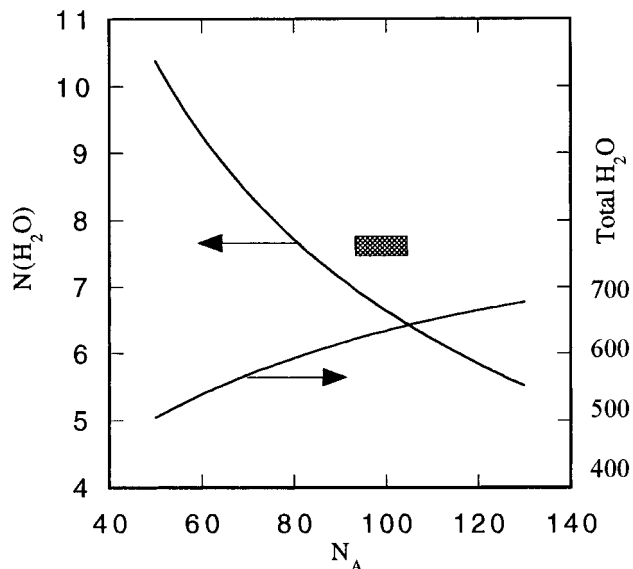


Figure 6. Number of water molecules per surfactant molecule $N(\text{H}_2\text{O})$ (left-hand ordinate) and the total water associated with the micelle (right-hand ordinate) as a function of the aggregation number N_A . The curves correspond to fixing $V_{\text{dry}} = 127 \text{ \AA}^3$, i.e., are derived from the center curve in Figure 5. The rectangle represents estimates of $N(\text{H}_2\text{O})$ from the hydrodynamic data of Tokiwa and Ohki.⁵⁰ The horizontal extent of the rectangle corresponds to a range of N_A , and the vertical extent spans the difference in two methods to estimate $N(\text{H}_2\text{O})$. Mukerjee's theoretical estimate based on only primary solvation of the ions is $N(\text{H}_2\text{O}) = 5$, near the lower limit of the present observations at the sphere-rod transition.

is constant. Therefore, the polarity index is predicted to decrease with N_A according to eqs 10, 11, and 14. These results are plotted as solid lines in Figure 5 together with the experimental results of two of the typical experiments. The numbers near each solid line denote the value of $N(\text{H}_2\text{O})$ at $N_A = 63$ for that line. Clearly, the theoretical curve for $N(\text{H}_2\text{O}) = 9$ at $N_A = 63$ is in excellent agreement with the experimental results.

The hydration number may be calculated by combining eqs 10, 11, and 13. These hydration numbers vary with micelle size as plotted in Figure 6 for the case of $V_{\text{dry}} = 127 \text{ \AA}^3$. The total water associated with the micelle may be calculated by multiplying the hydration number per surfactant molecule by the aggregation number; i.e., total water = $N_A N(\text{H}_2\text{O})$. The total water versus micelle size is also plotted in Figure 6 using the right-hand ordinate. The filled rectangle in Figure 6 represents the hydration numbers estimated by Tokiwa and Ohki⁵⁰ from measurements of sedimentation, diffusion, viscosity, and density of SDS in the concentration range from cmc to 87 mM in 100 mM NaCl. Of the various investigations^{49–51} of SDS, the data of these authors seem to be the most appropriate for the following reasons. First, their choice of 100 mM NaCl is an excellent compromise between the need to reduce the electroviscous effect and the need to have small enough micelles in order to assume a spherical shape. One must separate the effects of shape and hydration in order to derive a hydration number from hydrodynamic measurements.^{49–51} Second, holding [NaCl] constant at 100 mM and varying [SDS] from the cmc to 87 mM means that the aggregation number varies only by about 6% about the central value of $N_A = 98$. This minimizes the problem of not taking into account the variation of $N(\text{H}_2\text{O})$ with micelle size. The horizontal extent of the rectangle in Figure 6 represents the range of N_A in their measurements. Third, Tokiwa and Ohki⁵⁰ estimated the hydration numbers in two ways: (a) from sedimentation and diffusion data and (b) from reduced viscosity data, finding good agreement between the two

methods. The top and bottom of the rectangle in Figure 6 correspond to these two different methods to estimate the hydration number.

We emphasize that the numerical values of $H(25 \text{ }^\circ\text{C})$ and $N(\text{H}_2\text{O})$ predicted by eqs 9–14 are dependent on the model employed for the micelle as well as the numerical values of the parameters, notably N_c and the thickness of the polar shell. Therefore, Figure 5 ought not to be taken to prove that a hydration number at $N_A = 63$ of $N(\text{H}_2\text{O}) = 9$ is better than, say, $N(\text{H}_2\text{O}) = 8$. The important point is that, after fixing one parameter, a simple model with reasonable assumptions gives the rate of decrease of polarity with micelle size consistent with experimental results.

Discussion

Relative Aggregation Numbers. The micropolarity sensed by the 5DSE probe depends directly on the aggregation number of the SDS micelle and not on the ionic strength of the solution. This is demonstrated by the fact that for a given value of N_A attained using different combinations of [NaCl] and [SDS], the method yields the same value of A_0 . This means that the polarity of the surface of the micelle is independent of [NaCl] except through the salt's role in determining N_A . The micropolarity for a given value of N_A is also independent of the number of micelles in solution within the limits of these experiments; i.e., interactions between micelles do not affect the surface polarity. The limits are considerable. Consider, for example, the two points in Figure 3 near $N_A = 99$, corresponding to [SDS] = 500 mM and [NaCl] = 0 versus [SDS] = 50 mM and [NaCl] = 118 mM, respectively. These two points correspond to [micelles] = 5.0 and 0.5 mM, respectively. At the higher SDS concentration, the micelles are getting to be quite crowded. By use of a simple cubic lattice, the center-to-center micelle distance is 69 Å, compared with twice the micelle radius $2R_m = 50.4 \text{ \AA}$.

For a change in aggregation number, δN_A , eq 6 yields a change in hyperfine coupling constant, δA_0

$$\delta A_0 = \frac{\partial A_0}{\partial N_A} \delta N_A \quad (15)$$

For 5DSE, $\partial A_0 / \partial N_A = -3.99 \pm 0.02 \text{ mG/molecule}$, and since the spacing between hyperfine lines of 5DSE can be measured with a precision of 1–3 mG, this means that relative values of N_A may be determined from eq 15 to about one molecule per micelle. The precision with which absolute values of N_A may be determined is limited in almost all cases to the accuracy to which these aggregation numbers are known and not by the experimental uncertainties in the measurement of A_0 . The only exception arises when one attempts to measure A_0 in solutions very near the cmc where the uncertainties discussed in the Appendix could enter. We achieve high precision in the measurements of A_0 even in rather noisy spectra by fitting the spectra to a Voigt line shape. Without fitting, it is not difficult to achieve precisions on the order of 0.01 G on spectra showing good signal-to-noise ratios, but this can increase to 0.03 G on noisy spectra. With these latter spectra, the uncertainty in relative values of N_A reaches about eight molecules, still sufficient for some purposes. Relying on a Hall probe calibrated sweep range is probably adequate for relative values of A_0 (relative values of N_A); however, absolute values can be in serious error. For example, with our unit, a 50 G sweep range corresponds to about 50.2 G, which gives an error of about 0.06 G in A_0 , i.e., an uncertainty in the absolute value of N_A of 15 molecules.

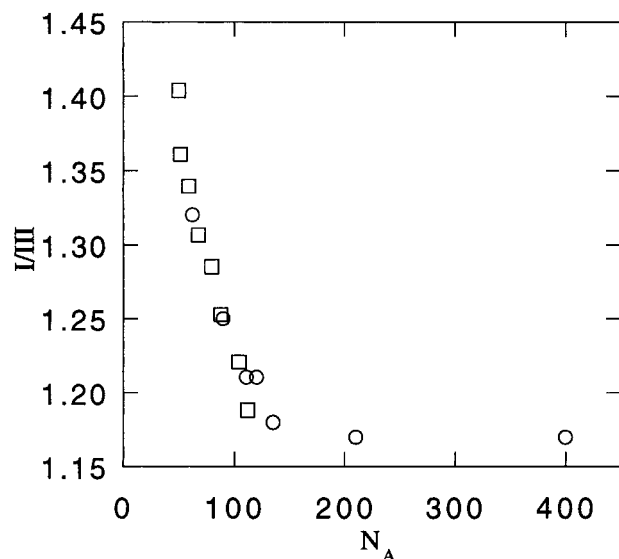


Figure 7. Intensity ratios of the first over the third peak in the fluorescence spectrum of pyrene as a function of the aggregation number N_A . Data from the literature are obtained by varying the concentration of NaCl in a 70 mM SDS solution³⁸ (O) or by varying the SDS concentration in the absence of salt⁵⁷ (□). The data are scaled to account for instrumental differences. See text.

The physicochemical properties of micelles change rather subtly with size, making them difficult to study by many more direct techniques. Although the present approach suffers from being indirect, it does offer a simple, precise method to look for small changes in N_A .

In particular, the potential to study subtle effects of (small amounts) of various additives is interesting. The influence of a number of additives on the aggregation numbers of SDS micelles has already been studied by Almgren and co-workers^{5,53,54} using time-resolved fluorescence quenching (TRFQ). Particularly interesting will be long-chain alcohols where presumably the OH group of the alcohol would enter into the calculation of the polarity.

It will be very interesting to see if this method is capable of detecting the small changes in N_A with temperature.^{1,2,26} As a practical matter, the interference of spin exchange as described in the Appendix would need to be treated with care because the spin exchange frequency is strongly temperature-dependent.⁵⁵

Further Evidence That the Micropolarity of SDS Micelles Decreases with Increasing Size. There is ample literature that exploits the solvent-dependent properties of various probes in order to study the polarity of SDS micelles (see, for example, ref 56, especially S.Table 2 of the Supporting Information). The model advanced here predicts that any molecule possessing solvatochromic properties residing for a significant fraction of the time near the micelle surface ought to show a decrease in polarity as the micelles grow. To our knowledge, the only such property that has been systematically studied as a function of micelle size is the so-called I/III ratio in the fluorescence emission spectrum of pyrene.^{38,57} Figure 7 shows data taken from the literature plotted as a function of the aggregation number. In Figure 7, the data of Lianos and Zana,³⁸ denoted by circles, were obtained by varying the concentration of NaCl in a 70 mM SDS solution and the values of N_A are those measured by the same authors³⁸ employing TRFQ measurements of the pyrene excimer. The data of Siemiarczuk and Ware,⁵⁷ represented by squares, were obtained by varying the SDS concentration in the absence of salt where the values of N_A are

computed from eq 5. The I/III ratio is known to generally decrease with decreasing polarity, so the data in Figure 7 may be interpreted as a decrease in polarity as the micelles grow.³⁸ Unfortunately, the values of the ratio I/III are not well reproduced by different labs, a problem that has been attributed to instrumental differences.⁵⁸ For example, measurements of the ratio for pyrene in water from various labs⁵⁸ lead to a standard deviation of about 9%, while reproducibility is about 1–2%.⁵⁸ In view of this, the data of Siemiarczuk and Ware⁵⁷ have been scaled upward by 8% so that the salt-free datum of Lianos and Zana³⁸ lies on the interpolation between two salt-free data points of Siemiarczuk and Ware.⁵⁷ This places the two data sets on the same footing; however, the absolute value of the ordinate is uncertain by about 8%. Deriving an estimate of the polarity from the I/III ratio involves further difficulties, since there is a lack of understanding about the probe solvent interactions.⁵⁸ Plots of the I/III ratio vs the polarity parameter $H(25\text{ }^\circ\text{C})$, for example, show poor correlation.⁵⁸ Thus, with the present precision in the measurements of the I/III ratio and the lack of a sound theory with which to proceed to a nonempirical polarity scale, not much more can be done with the data in Figure 7; nevertheless, the similarity in Figures 7 and 3 is compelling indeed. The conclusion is that the polarity decreases with micelle size when measured with a very different molecule, pyrene rather than 5DSE, using a different polarity parameter, and that the rate of decrease is similar whether NaCl or SDS is varied. In practical terms, the I/III ratio would not be a very suitable avenue to study relative micelle sizes.

In principle, the optical spectra of the nitroxide probes could be used to pursue the same kind of studies presented here; however, in practice, rather large concentrations of the probe are required.^{16–18} The relative precision^{16–18} of the optical measurements is about 0.3 nm/51 nm \approx 0.006 compared with \sim 0.001 for EPR measurements of A_0 . EPR enjoys the further advantage of not requiring sample transparency that might hinder optical measurements.

Hydration of the SDS Micelle Surface. The hydration model predicts, strictly on a geometric basis, a drying of the micelle surface (per surfactant molecule) as the micelle grows because less water will fit within the polar shell. Credit for this basic idea ought to go to Lianos and Zana.³⁸ We consider the model to be a success because it predicts the slope of the polarity vs aggregation number in good agreement with experimental results in Figure 5. The rather remarkably good fit between theory and experiment in Figure 5 is perhaps fortuitous given the simplicity of the model. Furthermore, the quantitative transformation from measured values of A_+ to values of the polarity index, $H(25\text{ }^\circ\text{C})$ involves an uncertainty (discussed below) of the effect of ions. This uncertainty could shift the experimental points in Figure 1 up or down; however, the slope is probably not affected very much. Thus, at this stage, one cannot rely on the absolute values of $N(\text{H}_2\text{O})$; however, it does seem clear that a decrease in values of $N(\text{H}_2\text{O})$ as the micelle grows is a viable working hypothesis. The predicted behavior of $H(25\text{ }^\circ\text{C})$ vs N_A is quite sensitive to the assumed value of the hydration number per surfactant molecule, as can be seen by comparing the curves in Figure 5 that differ by only one water molecule or less.

The model ought to be rather easily extended to micelles formed from surfactants of any charge state, provided that a spherical shell model is approximately correct. If this proves to be true, then measurements of A_0 will lead to precise relative aggregation number determinations for many micelles. In

practical terms, the method provides a means to monitor relative micelle sizes as experimental conditions are varied.

The model is consistent with the leveling of the polarity at the sphere-rod transition point evident in Figure 5 near $N_A = 130$. Although the micelle continues to grow, in fact, much faster than the abscissa indicates above $N_A = 130$, since eq 5 no longer applies above the transition, the volume per headgroup is not expected to vary much if the general picture of an elongating rod is correct.

The total water associated with the micelle increases as shown in Figure 6 (right-hand ordinate). The total water varies only by $\pm 15\%$ about its midpoint value, so although the drying per surfactant molecule is rather severe, the overall hydration change is more modest. This means that any method to determine $N(\text{H}_2\text{O})$ versus N_A based on a measurement of the total water associated with the micelle would need to be rather precise.

We have presented the hydration of the micelle surface as a geometric phenomenon with the counterion concentration entering indirectly as the agent that determines the micelle size (eq 1). A decrease in values of $N(\text{H}_2\text{O})$ as the micelle grows also seems physically reasonable from another point of view if we view the micelle as two "phases" and draw upon the analogy with ion-exchange resins.⁵⁹ These resins swell with water around the charged ionogenic centers in an attempt to equalize the concentration (activity) of the ions in the resin and in the aqueous phase (see, for example, chapter 5 of ref 59). The swelling is driven by the osmotic pressure difference between the two "phases" and is opposed by the mechanical pressure from the interchain cross-links. The interplay between the swelling pressure and the mechanical pressure determines the equilibrium water content. If the ion concentration is increased by adding salt, the ion concentration difference in the two phases decreases, reducing the swelling pressure and leading to a lower water concentration. In ionic micelles, the hydrophobic effect provides the force that limits the "swelling". For increasing values of $[\text{Na}^+]_{\text{aq}}$, furnished either by higher detergent concentrations or by added salt, the diminished concentration difference would decrease the osmotic pressure, leading to a dehydration (per surfactant molecule) of the micelle surface.⁶⁰

The agreement between the values of $N(\text{H}_2\text{O})$ derived from spin-probe measurements and the theoretical model and those from transport data, represented by the rectangle in Figure 6, supports the idea that the number of water molecules that move as a kinetic unit with the SDS micelle is the same as the number of water molecules that are housed in the polar shell and enter into our model. This supports the contention of Mukerjee⁴⁹ who suggested that additional hydration layers were not important. Our model is different in detail than that envisioned by Mukerjee⁴⁹ in that $N(\text{H}_2\text{O})$ varies with micelle size. Mukerjee's⁴⁹ theoretical estimate of $N(\text{H}_2\text{O}) = 5$, using primary hydration numbers of 4 and 1 for Na^+ and the sulfate headgroup, respectively, is smaller than our values (Figure 6) except near the sphere-rod transition. To the extent that our values of $N(\text{H}_2\text{O})$ in Figure 6 hold up under further investigation and that taking Mukerjee's⁴⁹ estimate of $N(\text{H}_2\text{O}) = 5$ to be reasonable means that some of the water in the polar shell is "free" over most of the range of N_A . We do not yet know if it is significant, but the sphere-rod transition occurs at about the point that "free" water disappears in our model, since the primary hydration of 5 is near our estimate of $N(\text{H}_2\text{O}) = 5.5$ at this transition.

In the model, it was supposed that the nitroxide moiety sampled all of the polar shell and only the polar shell. The fact that the model gives reasonable results for $N(\text{H}_2\text{O})$ supports

this view. The spin probe 5DSE is quite hydrophobic except for the NO group. It seems reasonable that the hydrophilic NO group of 5DSE resides in the polar shell because, in order for the group to range very far outside the polar shell, either the hydrophobic moieties attached to the NO group would have to be dragged into the hydrophilic region or the hydrophilic NO group would have to reside in the hydrophobic region, contrary to the findings of Mukerjee and co-workers.¹⁸ Nevertheless, any rapid motion involving excursions of the NO group into the hydrocarbon core and into the aqueous region would involve averaging values of $H(25^\circ\text{C})$ near unity and zero, respectively, and would be difficult to detect. For example, excursions of equal probability into these regions would yield $H(25^\circ\text{C}) = 0.5$, which would have to be averaged, with the appropriate statistical weight, with the values of $H(25^\circ\text{C})$ appropriate to the polar shell. It is clear from Figure 5 that such excursions would affect the reported polarity minimally, since $H(25^\circ\text{C}) = 0.5$ is near the values reported.

The remarks in the previous paragraph would apply to any spin probe composed only of hydrophobic moieties except for the NO group. In particular, the entire series of doxylstearic acid esters with the doxyl attached at various carbon atoms ought to have about the same polarity in an SDS micelle. In contrast, the doxylstearic acids, particularly those labeled near the charged carboxyl group, would possess an additional hydrophilic moiety that would be expected to alter the average location of the NO group, possibly leading to different results.

Testing of the Model

The model predicts that only the volume fraction occupied by water in the polar shell is important. Within the caveat of the following paragraph, this means that the presence of counterions has only the secondary effect of occupying volume in the polar shell of the micelle. Thus, exchanging Li^+ for Na^+ in SDS is predicted to have only a minor effect if micelles of the same size are compared. It is important to note that in developing the model, we have not distinguished between "free" water and waters of solvation associated with the cations (see p 104 of ref 59). We have made the tacit assumption that the polarity index $H(25^\circ\text{C})$ does not distinguish between the two types of water; therefore, at this level of sophistication, it does not matter that a hydrated Li^+ ion is probably larger than a hydrated Na^+ ion, since we are accounting for the total water in the polar shell. Thus, we predict that the value of A_0 for a given value of N_A would not depend on the counterion because, although the two ions have different sizes, neither occupies much volume. Note, however, that for a given value of the right-hand side of eq 5, one finds a smaller value of N_A for lithium dodecyl sulfate than for SDS.³⁷ In contrast, if a much larger counterion were employed, e.g., trimethylammonium (140 \AA^3),⁵² the space-filling aspect might be detectable. Obviously, in every case, an independent measurement of the aggregation number is needed in order to study A_0 vs the aggregation number.

In aqueous and methanolic solutions, dissolved salts have been found to produce small changes in the values of A_0 for small, neutral, water soluble spin probes.^{16,23} We have neglected such effects and in discussing the anticipated results using Li^+ in place of Na^+ , we have assumed that such effects would not depend on the replacement of one of these ions by the other.

Another aspect of the lithium versus sodium counterion experiments can be easily tested. The sphere-rod transition thought to occur in sodium dodecyl sulfate does not occur in lithium dodecyl sulfate even up to salt concentrations of 0.81 M.³⁷ According to the model, one does not expect a leveling of the value of A_0 (or A_+ or H) at high Li^+ concentrations.

A severe test of the model would come from studies of the rest of the normal sodium alkyl sulfates with carbon chain lengths from 8 to 11. The model predicts that A_0 would be the same under conditions in which the volume in the polar shell per surfactant molecule V_p were the same, provided the inaccessible volume V_{dry} were the same. Even with the uncertainties surrounding the simple model, it is reasonable to assume that the details of the polar region would be similar, since they house the same headgroup. Therefore, a plot of A_+ versus V_p is predicted to be a universal curve *with no adjustable parameters*, not even V_{dry} . Even the question of whether N_c ought to be the total number of carbon atoms or less than the total would not affect the results very much as long as consistency is maintained throughout the series. N_A could be varied with various combinations of surfactant and salt concentration; thus, the universal curve could be tested over quite wide ranges of N_A .

Conclusions

The polarity of SDS micelles sensed by the spin probe 5DSE depends on the micelle aggregation number only, not on the combination of surfactant and salt concentrations. One-half the difference in the high- and low-field resonance fields, A_0 , varies linearly with N_A according to eq 6; thus, the absolute value of N_A may be determined with a precision limited only by its known value, while relative values of N_A may be determined to within about one molecule. These conclusions do not depend on the use of the empirical equation eq 5. A model describing the hydration of the micelle surface as a function of micelle size is advanced that is in excellent agreement with experimental observations employing only one adjustable parameter, the hydration number per surfactant molecule at a given value of N_A . Once this parameter is fixed, the hydration number per surfactant molecule decreases with N_A . The model may be subjected to severe future experimental tests.

Acknowledgment. This work was supported by grants from the Fundação de Amparo À Pesquisa do Estado de São Paulo (FAPESP Project 94/1111-8), the NIH/MBRS S06 GM48680-03, and the CSUN Research and Grants Committee (to BB and M.P.). A.V. was supported as a MBRS Undergraduate Research Assistant.

Appendix. Dependence of A_0 upon Spin-Probe Concentration

Spin exchange between spin-probe molecules leads to the well-known effect of shifting the outer lines toward the center,^{55,61} which would appear as an apparent decrease in A_0 according to our operational definition. In a micellar solution, to obtain correct spin exchange frequencies from the observed shifts, proper account for the distribution of the spin probe among the micelles must be taken (see eqs 12–15 of ref 62 and references therein for discussions of the problem). Briefly, micelles containing one spin probe yield unshifted spectra, those containing two yield a shift, those containing three yield a larger shift, etc. There are spin statistics as well as micelle distribution statistics involved, and subtle matters such as the fact that the spin exchange frequency is expected to be smaller in a larger micelle. For the purpose at hand, this kind of detail is unnecessary, since we wish to correct for the shift rather than deduce the spin exchange frequencies. We make the standard assumption⁵⁵ that the spin exchange frequency is proportional to the molar ratio of 5DSE to micellized SDS, X_m . Assuming that all of the 5DSE is associated with the micelles, $X_m =$

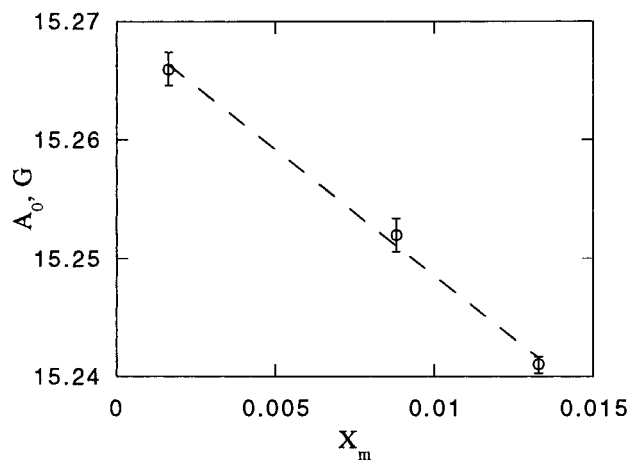


Figure 8. One-half the difference in the resonance fields of the high- and low-field lines of 5DSE in 50 mM SDS vs the mole fraction of 5DSE to micellized SDS. The decrease in A_0 versus X_m is due to spin exchange interactions that shift the outer lines toward the center.

$[5DSE]/([SDS] - [SDS]_{free})$. Usually, experiments are carried out with constant molar ratios of spin probe to surfactant, $X = [5DSE]/[SDS]$, which is related to X_m as follows:

$$X_m = X/(1 - [SDS]_{free}/[SDS]) \quad (16)$$

For most applications, it is rather easy to design experiments with quite small values of X . By selection of modulation amplitudes on the order of the EPR line width²⁹ and microwave powers that lead to slight power saturation and by use of least-squares fitting techniques,¹⁴ accurate results may be obtained from samples of concentration as low as 10^{-5} M. This means, for example, that for an experiment with $[SDS]$ near the cmc_0 of 8.3 mM, a value of X as low as $X = 1.2 \times 10^{-3}$ may be quickly attained with no need for signal averaging.

Figure 8 shows A_0 versus X_m for a 50 mM SDS solution with no additional salt. The solid line is a linear least-squares fit yielding

$$A_0 = 15.270 - 2.13X_m, \quad r = 0.998 \quad (17)$$

The second term is the shift due to spin exchange. Combining eqs 17 and 6 shows that an error of about one molecule results from $X_m = 0.002$. To apply the correction, X is calculated from the experimental preparation, $[SDS]_{free}$ from eq 5 of ref 8, and X_m from eq 16 and $2.13X_m$ is added to the observed value of A_0 . This correction may be calculated for each sample in a series; however, the correction often will be the same for each member of the series. This occurs for experiments that employ a constant value of X , and $[SDS]_{free}/[SDS]$ either is negligible or does not vary significantly. In either case, X_m is approximately constant. For these cases, even if the correction in eq 17 is not negligible, only the value of $A_0(0)$ is affected, not the value of $\partial A_0/\partial N_A$.

References and Notes

- (1) Croonen, Y.; Geladé, E.; Van der Zegel, M.; Van der Auweraer, M.; Vandendriessche, H.; De Schryver, F. C.; Almgren, M. *J. Phys. Chem.* **1983**, *87*, 1426.
- (2) Bezzobotnov, V. Y.; Borbély, S.; Cser, L.; Faragó, B.; Gladkih, I. A.; Ostanevich, Y. M. *J. Phys. Chem.* **1988**, *92*, 5738.
- (3) Bales, B. L.; Almgren, M. *J. Phys. Chem.* **1995**, *99*, 15153.
- (4) Gehlen, M. H.; De Schryver, F. C. *J. Phys. Chem.* **1993**, *97*, 11242.
- (5) Almgren, M.; Swarup, S. *J. Phys. Chem.* **1982**, *86*, 4212.
- (6) Huisman, H. F. *Proc. K. Ned. Akad. Wet.* **1964**, *B67*, 367.
- (7) Sasaki, T.; Hattori, M.; Sasaki, J.; Nukina, K. *Bull. Chem. Soc. Jpn.* **1975**, *48*, 1397.

- (8) Quina, F. H.; Nassar, P. M.; Bonilha, J. B. S.; Bales, B. L. *J. Phys. Chem.* **1995**, *99*, 17028.
- (9) Bales, B. L.; Stenland, C. *Chem. Phys. Lett.* **1992**, *200*, 475.
- (10) Bales, B. L.; Stenland, C. *J. Phys. Chem.* **1993**, *97*, 3418.
- (11) Lamaire, H.; Rassat, A. *J. Chim. Phys. Phys.-Chim. Biol.* **1964**, *61*, 1580.
- (12) Mukai, K.; Nishiguchi, H.; Ishizu, K.; Deguchi, Y.; Jakaki, H. *Bull. Chem. Soc. Jpn.* **1967**, *40*, 2731.
- (13) Griffith, O. H.; Dehlinger, P. J.; Van, S. P. *J. Membr. Biol.* **1974**, *15*, 159.
- (14) Halpern, H. J.; Peric, M.; Yu, C.; Bales, B. L. *J. Magn. Reson.* **1993**, *103*, 13.
- (15) Smirnov, A. I.; Belford, R. L. *J. Magn. Reson.* **1995**, *A113*, 65.
- (16) Ramachandran, C.; Pyter, R. A.; Mukerjee, P. *J. Phys. Chem.* **1982**, *86*, 3198.
- (17) Mukerjee, P.; Ramachandran, C.; Pyter, R. A. *J. Phys. Chem.* **1982**, *86*, 3189.
- (18) Pyter, R. A.; Ramachandran, C.; Mukerjee, P. *J. Phys. Chem.* **1982**, *86*, 3206.
- (19) Schwartz, R. N.; Peric, M.; Smith, S. A.; Bales, B. L. *J. Phys. Chem. B* **1997**, *101*, 8735.
- (20) Knauer, B. R.; Napier, J. J. *J. Am. Chem. Soc.* **1976**, *98*, 4395.
- (21) Reddock, A. H.; Konishi, S. *J. Chem. Phys.* **1979**, *70*, 2121.
- (22) Abe, A.; Ogino, K. **1982**, *31* (9), 141.
- (23) Jackson, S. E.; Smith, E. A.; Symons, M. C. R. *Discuss. Faraday Soc.* **1978**, *64*, 173.
- (24) Abe, T.; Tero-Kubota, S.; Ikegami, Y. *J. Phys. Chem.* **1982**, *86*, 1358.
- (25) Siemiarczuk, A.; Ware, W. R.; Liu, Y. S. *J. Phys. Chem.* **1993**, *97*, 8082.
- (26) Malliaris, A.; Le Moigne, J.; Sturm, J.; Zana, R. *J. Phys. Chem.* **1985**, *89*, 2709.
- (27) Bales, B. L.; Wajnberg, E.; Nascimento, O. R. *J. Magn. Reson.* **1996**, *A118*, 227.
- (28) Peric, M.; Halpern, H. J. *J. Magn. Reson. A* **1994**, *109*, 198.
- (29) Bales, B. L.; Peric, M.; Lamy-Freund, M. T. *J. Magn. Reson.* **1998**, *132*, 279.
- (30) Sartori, J. C.; Nascimento, O. R. *Rev. Fis. Apl. Instrum.* **1992**, *7*, 115.
- (31) Polnaszek, C. F.; Freed, J. H. *J. Phys. Chem.* **1975**, *79*, 2283.
- (32) Hwang, J. S.; Mason, R. P.; Hwang, L.-P.; Freed, J. H. *J. Phys. Chem.* **1975**, *79*, 489.
- (33) Rao, K. V. S.; Polnaszek, C. F.; Freed, J. H. *J. Phys. Chem.* **1977**, *81*, 449.
- (34) Fraenkel, G. K. *J. Chem. Phys.* **1965**, *42*, 4275.
- (35) Bales, B. L.; Mareno, D.; Harris, F. L. *J. Magn. Reson. A* **1993**, *104*, 37.
- (36) Doughty, D. A. *J. Phys. Chem.* **1979**, *83*, 2621.
- (37) Berr, S. S.; Jones, R. M. *Langmuir* **1988**, *4*, 1247.
- (38) Lianos, P.; Zana, R. *J. Phys. Chem.* **1980**, *84*, 3339.
- (39) Hayashi, S.; Ikeda, S. *J. Phys. Chem.* **1980**, *84*, 744.
- (40) Mazer, N. A.; Benedek, G. B.; Carey, M. C. *J. Phys. Chem.* **1976**, *80*, 1075.
- (41) Lindman, B.; Wennerström, H.; Gustavsson, H.; Kamenka, N.; Brun, B. *Pure Appl. Chem.* **1980**, *52*, 1307.
- (42) Bales, B. L.; Stenland, C. *J. Phys. Chem.* **1995**, *99*, 15163.
- (43) Cabane, B.; Duplessix, R.; Zemb, T. *J. Phys.* **1985**, *46*, 2161.
- (44) Cabane, B. *Small-Angle Scattering Methods. In Surfactant Solutions. New Methods of Investigation*; Zana, R., Ed.; Marcek Dekker: New York, 1987; Vol. 22, p 57.
- (45) Berr, S. S.; Caponetti, E.; Johnson, J. S., Jr.; Jones, R. R. M.; Magid, L. J. *J. Phys. Chem.* **1986**, *90*, 5766.
- (46) Berr, S. S. *J. Phys. Chem.* **1987**, *90*, 5766.
- (47) Berr, S.; Jones, R. R. M.; Johnson, J. S., Jr. *J. Phys. Chem.* **1992**, *96*, 5611.
- (48) Tanford, C. *The Hydrophobic Effect: Formation of Micelles and Biological Membrane*, 2nd ed.; Wiley-Interscience: New York, 1980.
- (49) Mukerjee, P. *J. Colloid Sci.* **1964**, *19*, 722.
- (50) Tokiwa, F.; Ohki, K. *J. Phys. Chem.* **1967**, *71*, 1343.
- (51) Courchene, W. L. *J. Phys. Chem.* **1964**, *68*, 1870.
- (52) Berr, S. S.; Coleman, M. J.; Jones, R. R. M.; Johnson, J. S., Jr. *J. Phys. Chem.* **1986**, *90*, 6492.
- (53) Almgren, M.; Swarup, S. *J. Colloid Interface Sci.* **1983**, *91*, 256.
- (54) Almgren, M.; Swarup, S. *The Size of Sodium Dodecyl Sulfate Micelles with Various Additives: A Fluorescence Quenching Study. In Surfactants in Solution*; Lindman, K. L. M. a. B., Ed.; Plenum: New York, 1984; Vol. 1; p 613.
- (55) Molin, Y. N.; Salikhov, K. M.; Zamarayev, K. I. *Spin Exchange. Principles and Applications in Chemistry and Biology*; Springer-Verlag: New York, 1980; Vol. 8.
- (56) Grieser, F.; Drummond, C. J. *J. Phys. Chem.* **1988**, *92*, 5580.
- (57) Siemiarczuk, A.; Ware, W. R. *Chem. Phys. Lett.* **1990**, *167*, 263.
- (58) Konuk, R.; Cornelisse, J.; McGlynn, S. P. *J. Phys. Chem.* **1989**, *93*, 7405.
- (59) Helfferich, F. *Ion Exchange*; McGraw-Hill: New York, 1962.
- (60) Quina, F. H. This interpretation was suggested to us by Frank Quina of the Universidade de São Paulo.
- (61) Bales, B. L.; Peric, M. *J. Phys. Chem. B* **1997**, *101*, 8707.
- (62) Persson, K.; Bales, B. L. *J. Chem. Soc., Faraday Trans.* **1995**, *91*, 2863.